Microchimica Acta (2022) 189: 26
https://doi.org/10.1007/s00604-021-05131-2

ORIGINAL PAPER

A sensitive electrochemical sensor based on metal cobalt wrapped conducting polymer polypyrrole nanocone arrays for the assay of nitrite

Haitao Lü[1] · Hao Wang[1] · Lili Yang[1] · Yan Zhou[1] · Lixiao Xu[2] · Ni Hui[1] · Dongwei Wang[1]

Received: 18 September 2021 / Accepted: 6 December 2021 / Published online: 14 December 2021

Abstract

The conducting polymer polypyrrole nanocones wrapped by metal cobalt (Co/PPy) are a promising platform for the detection of sodium nitrite, which can be obtained by an electrochemical deposition technique under a mild condition. Co/PPy nanocone arrays combined the high conductivity and large specific surface area of PPy nanocones with the redox properties of metal cobalt, and their 3D structure can provide more active sites for nitrite detection. Owing to the microstructure and excellent electrical properties of the nanocomposite, Co/PPy nanocone arrays were convenient to construct a high-performance nitrite sensor. The microscopic morphology and composition of Co/PPy nanocone arrays were characterized by SEM, FT-IR, XPS, and XRD, and their electrochemical performances were also investigated. The experimental results showed that Co/PPy nanocones exhibited excellent performance for nitrite determination. The sensors were used for the determination of nitrite in pickled Chinese cabbage and water samples, and the results were consistent with those of spectrophotometry. Hence, the synthesized Co/PPy nanocone arrays have a broad application prospect in food safety, environmental protection, and industrial manufacturing.

Keywords Conducting polymer · Polypyrrole nanocone arrays · Cobalt nanoparticles · Nitrite determination · Electrochemical sensor · Amperometry

Introduction

Nitrite is the commonest nitrogen compounds with great significance in a lot of fields such as food preservatives, chemical synthesis, industrial manufacturing, environmental protection, meat coloring agents, and fabric dying [1–4]. Moreover, nitrite is similar in appearance and taste to salt, which often exists in vegetables, fruit, and grains, especially in cured meat and mustard [5]. Therefore, nitrite poisoning is mostly brought about by improper diet. If excessive intake of nitrite, it will cause hemoglobin to oxidize, leading to tissue hypoxia, and under certain conditions, carcinogens-nitrosamines can be obtained [5, 6]. In recent years, numerous analytical techniques have been used to determine nitrite, such as high-performance liquid chromatography, electrochemical methods, spectrophotometry, and Raman spectroscopy [7–11]. Among them, electrochemical techniques have been widely and continuously researched for monitoring nitrite owing to the rapid response, ease in sample preparation and analysis, high cost-effectiveness [12–15]. However, the bare plane electrodes usually tend to be contaminated by electroactive species and other coexisting substances in the sample. Fortunately, the use of conducting polymer-modified electrodes can effectively meet the ever growing demand [16].

Conducting polymers have been widely investigated for multitudinous applications in these fields such as sensors, energy storage devices [17], metal anti-corrosion [18,

Haitao Lü, Hao Wang and Lili Yang contributed equally to this work.

✉ Lixiao Xu
xulixiao78@163.com

✉ Ni Hui
huini1029@163.com

✉ Dongwei Wang
w88030661@163.com

[1] College of Chemistry and Pharmaceutical Sciences, Qingdao Agricultural University, Qingdao, China

[2] School of Pharmacy, Key Laboratory of Molecular Pharmacology and Drug Evaluation (Yantai University), Ministry of Education, Collaborative Innovation Center of Advanced Drug Delivery Systemand Biotech Drugs in Universities of Shandong, Yantai University, Yantai 264005, Shandong, China

19], electrocatalysis [20, 21], and supercapacitor [22, 23]. Among the conducting polymer family, polypyrrole (PPy) has been widely regarding as a shining star due to the distinctive characteristics of excellent electrochemical stability, excellent biocompatibility, high electrical conductivity, high specific capacitance, and environmental friendliness in the present era [24]. One-dimensional PPy nanomaterial (such as nanowire, nanocone, nanofiber) can be used as the substrate for the attachment of various metal nanomaterials due to its excellent ordered linear structure. Therefore, PPy nanowires modified with metal are anticipated to display new characteristics on the basis of their unique constituent, making them potential for nitrite sensor [25]. In practical applications, the composite materials, which can combine the excellent catalytic ability of metal nanomaterials with the excellent electrochemical properties of conducting polymers, have high sensitivity, good plasticity, and controllable conductivity [26, 27].

Cobalt nanomaterial has attracted much attention because of its outstanding electrochemical properties such as high specific surface area and more electroactive sites. In particular, its three-dimensional (3D) nanostructures is helpful for its application as catalysts, high-performance supercapacitors, and ionic battery materials [26]. Thus, it can be anticipated that the PPy nanowires modified with cobalt nanoparticles can deliver high capacitance, electrical conductivity, and excellent catalytic capability due to the synergistic effect of nanocomposite components [28–31].

In this study, we successfully synthesized one-dimensional PPy nanocone arrays by the help of sodium p-toluenesulfonate (pTos) as the soft template. Then, the cobalt nanoparticles (Co) were electrodeposited on PPy nanocone film using constant-potential method. Thus, hierarchical Co/PPy nanocone arrays were obtained. PPy nanocone arrays can provide large specific surface area for growing and scattering Co nanoparticles. As shown in Scheme 1, an ultrasensitive sensor for nitrite determination was developed through a simple, two-step strategy. Encouragingly, this hierarchical Co/PPy nanocone arrays combined salient properties of Co nanoparticles and the conducting polymer PPy, and the nanocomposite-modified electrode showed highly sensitive and stable electrochemical detection of nitrite. Moreover, the method was used for the determination of nitrite in real samples and satisfactory result was obtained.

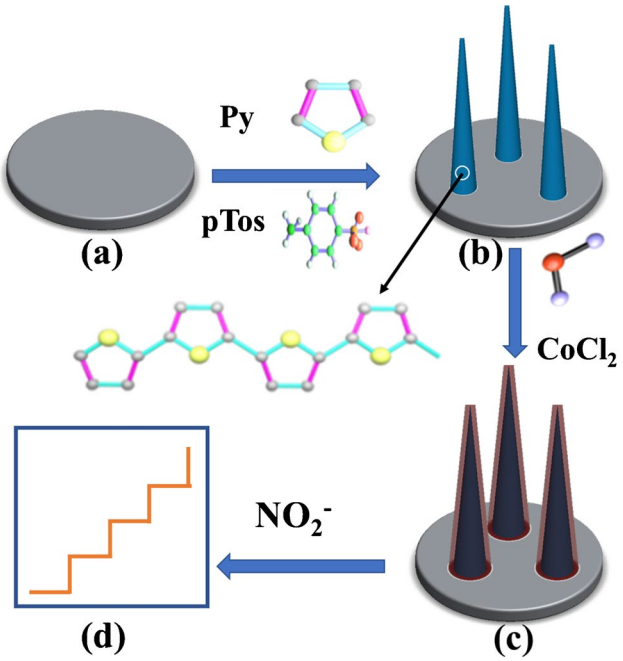

Scheme 1. Schematic diagram of the sensor based on Co/PPy nanocone arrays for the detection of nitrite. (a) Bare electrode, (b) PPy/GCE, (c) Co/PPy/GCE, and (d) the current response for the nitrite oxidation

Experimental

Reagents and instruments

Pyrrole, NaH_2PO_4, $Na_2HPO_4{\cdot}12H_2O$, and KCl were purchased from Aladdin regent (Shanghai, China). Sodium p-toluene sulfonate (pTos) was bought from Tianjin Bode Chemical Co. LTD (Tianjin, China). Cobalt chloride hexahydrate ($CoCl_2{\cdot}6H_2O$) and sodium nitrite ($NaNO_2$) were bought from Tianjin Beichen Founder Reagent Factory (Tianjin, China). Perchloric acid ($HClO_4$) was purchased in Tianjin Xinyuan Chemical Co., Ltd.

For the electrochemical tests, X-ray diffraction (XRD) patterns, scanning electron microscope (SEM), and X-ray photoelectron spectroscopy (XPS) analysis, all the required instruments (models) can refer to reference [32].

Fabrication of the Co/PPY-modified electrodes

Before use, the GCE were polished and cleaned according to the method reported in literature [33]. Co/PPY nanocones were prepared through the constant potential technique onto the GCE. Firstly, the PPy nanocones were electrodeposited on the surface of the GCE at a constant potential of 0.75 V in a 5.0-ml phosphate buffer solution (PBS pH 6.86) containing 0.15 M pyrrole and 0.1 M pTos for 600 s [34]. Then, the Co nanoparticles were electrodeposited onto the PPy nanocone surface at a constant potential of − 1.0 V in a 5.0 ml solution containing 10 mM $CoCl_2$ for 300 s. Co/PPy nanocomposite-modified GCE was denoted as Co/PPy/GCE.

Electrochemical measurements

The Co/PPy/GCE was tested as a nitrite sensor by CV and chronoamperometry in PBS (0.2 M, pH 8.0). CV measurements were carried out in the potential range of − 0.4 ~ 1.2 V. Chronoamperometry was carried out at a constant potential of 0.8 V. The background current reached a constant value before sodium nitrite was added, and the current curve was obtained by adding 10 µl sodium nitrite of different concentrations into the stirred solution. The galvanostatic charge and discharge tests were performed in a 2.0 M $HClO_4$ solution with different current densities (0.1, 0.3, 0.5, 0.7, 1.0, 1.5, 2.0 A g^{-1}).

Results and discussion

Formation of Co/PPy nanocomposite and characterizations

Surface morphologies of the synthetic PPy and the Co/PPy nanocone arrays were characterized by SEM. Figure 1(A and B) (low and high magnification images) shows the smooth surface of the synthetic PPy nanocones. The morphology of PPy exhibited an interleaved, inhomogeneous thickness nanocone structure. Due to the presence of a lot of voids in the nanocones, PPy nanocone arrays possessed high superficial area, which provided a faultless substrate for the attaching of cobalt nanoparticles. Furthermore, the intersecting

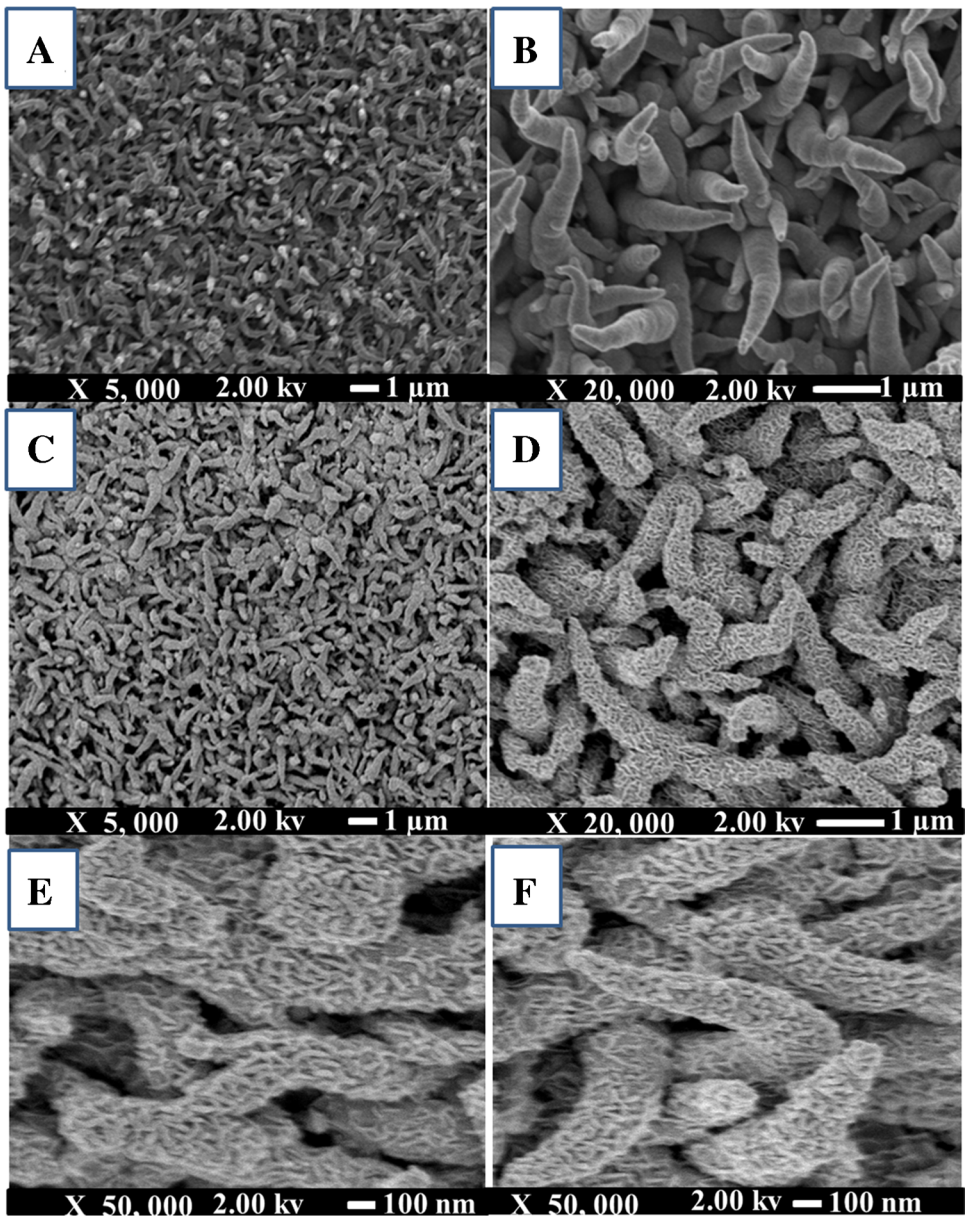

Fig. 1 SEM images of electrodes modified with (**A**, **B**) PPy nanocones and (**C**, **D**, **E**, **F**) Co/PPy nanocomposites

surface and lots of micropores mutually by the nanocones could provide electron transfer channels for nitrite oxidation. Figure 1(C–F) exhibits the morphology of Co/PPy nanocomposites. Cobalt nanoparticles were attached to the surface of PPy nanocones, interleaving along the PPy nanocones to form a hierarchical three-dimensional (3D) structure. Cobalt nanoparticles have almost covered the underlying PPy nanocones. The small diameter and homogeneous spread of cobalt nanoparticles provided numerous excellent properties, such as high surface-to-volume ratio, specific capacitance, and a great quantity of electroactive sites, which was beneficial to construct a sensitive nitrite sensor.

One-dimensional PPy nanomaterials prepared by template free method have attracted much attention due to their excellent advantages, such as simple synthesis, easy replication, environmental friendliness, and easy biological application. There were two common explanations for the formation mechanism of one-dimensional PPy. The first hypothesis is that amine of pyrrole interacted with hydrogen of $HPO_4^{2-}/H_2PO_4^-$ (used as electrolyte), to form hydrogen bond in the process of nucleation. The formation of PPy oligomers is due to their self-alignment, which leads to the formation of ordered bundle structure during the growth process, and finally to the formation of aligned PPy nanotubes [35]. In addition, another explanation has been provided, that is, the mechanism of self-assembled bubbles formed on the working electrode, which can be used as a chemical template for the growth of PPy [36]. In this work, PPy nanocones were successfully prepared by template free method, and the formation mechanism confirmed the first explanation.

The chemical states and elemental compositions of nanocomposites were studied through XPS. As illustrated in Fig. 2A (curve a), the XPS pattern of PPy nanocones exhibited strong signals at 284, 400, and 531 eV which are homologous to C (1 s), N (1 s), and O (1 s), respectively, which is the typical characteristic of PPy [37]. In the curve b, the peak at 780.80 eV appears which corresponds to the Co element. XPS analysis of Co region for Co/PPy was also obtained (Figure S1). Atomic composition of PPy and Co/PPy nanocone-modified electrodes is showed in Table S1. The XPS results provided direct evidence of the presence of Co in the nanocomposites [38]. Concurrently, the experimental results confirmed that the Co/PPy has been successfully prepared.

XRD was performed to characterize the nanostructures and compositions of the PPy nanocones and Co/PPy nanocomposites. As shown in Fig. 2B (both curve a and curve b), the scattering of PPy chain at the crystal plane spacing leads to a wide amorphous diffraction peak at 25°. Only in curve b, three major peaks at 43.5°, 50.5, and 74.5°can be observed which can be attributable to the diffraction from the (111), (200), and (220) planes of Co, respectively [29]. Therefore, this result was consistent with that of XPS and proved the successful preparation of Co/PPy nanocomposites.

FT-IR spectroscopy is an efficient tool to analyze the structure property of PPy and Co/PPy. As shown in Figure S2, the main bands situate at 1597 cm^{-1} (the asymmetric C = C stretching vibrations in the PPy), at 1349 cm^{-1} (symmetric C = N stretching vibrations), at 1277, and 1078 cm^{-1} (C-H and C-N in-plane deformation modes) [39]. The deposition of Co nanoparticles onto PPy nanocones did not change the characteristic peaks of PPy, but greatly improved the absorbance value.

The electrochemical performance of the sensor mainly depended on the microstructure of the modified materials, that is, the active region they can supply. The electroactive surface areas of bare electrode, Co nanomaterials, PPy nanocones, and Co/PPy nanocomposite-modified electrodes were counted by chronocoulometry (CC) technique [37], which is an easy and fast method to estimate the electrochemical surface area of the electrodes. As shown in Fig. 3, the CC tests of four different modified electrodes were performed

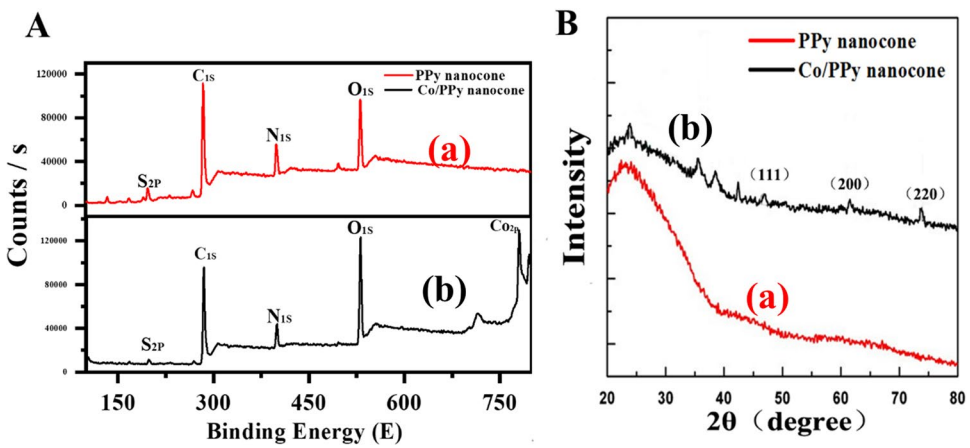

Fig. 2 (A) XPS spectra and (B) XRD spectra of PPy nanocone arrays (curve a) and Co/PPy nanocomposites (curve b)

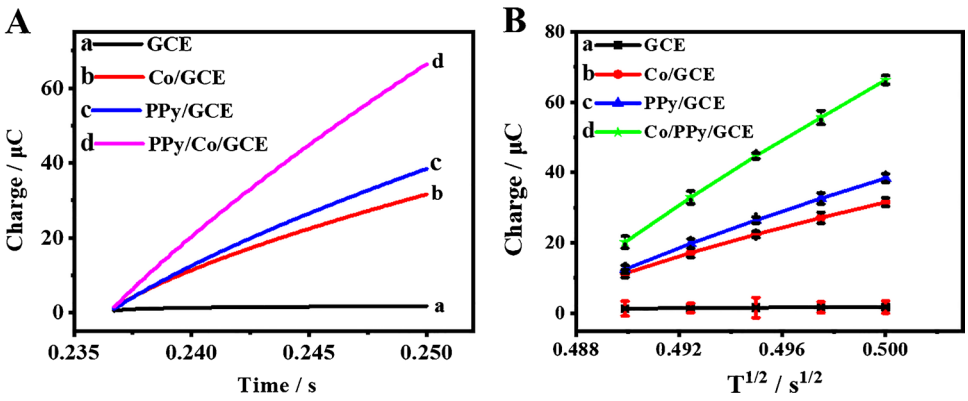

Fig. 3 (A) Chronocoulometric curves of (a) bare GCE, (b) PPy/GCE, and (c) Co/PPy/GCE in 5 mM $[Fe(CN)_6]^{4-/3-}$ containing 0.1 M KCl. (B)the relationship between Q and $t^{1/2}$. Error bar represents the deviation of three repeated determinations in this work

in the mixed solution of 5 mM $K_3Fe(CN)_6$ and 0.1 M KCl. According to the Cottrell equation $[Q(t) = (2nFAD^{1/2}\pi^{-1/2}C)t^{1/2} + Q_{dl} + Q_{ads}]$, the active surface area of the electrodes can be calculated by the slope of the Q-$t^{1/2}$ plots [40]. It was found that the slope of Co/PPy/GCE reached the maximum among the four electrodes, which meant that the active area of Co/PPy/GCE was the largest among them (curve d, Fig. 3B). The active surface area of the Co/PPy/GCE (curve d, 1.313 cm^2) was counted, which was 96, 3.05, and 2.15 times larger than that of the bare GCE (curve a, 0.0137 cm^2), the Co/GCE (curve b, 0.43 cm^2), and PPy/GCE (curve c, 0.61 cm^2), respectively. These results showed that both Co nanoparticles and PPy nanocone arrays can greatly expand the active surface area of the electrodes, while the Co/PPy nanocomposites had the largest active area due to the synergistic effect. Co/PPy/GCE can supply a large number of electroactive sites and a favorable platform for short channels for electrolyte ions and electrons.

CVs and galvanostatic charge–discharge tests were performed to investigate the capacitance on the nanocomposites [31]. Figure S3A shows that the specific capacitances of the Co/PPy/GCE and PPy/GCE are calculated and compared at the same current density (1A g^{-1}) in 2.0 M $HClO_4$. Co/PPy/GCE nanocomposite had large curve time span, indicating that the specific capacitance of the Co/PPy/GCE was much higher than that of the pure PPy/GCE. CV curve of Co/PPy/GCE maintained the largest area under the curve, also showing its superior supercapacitive property than that of the PPy nanocone arrays (the inset curve in Figure S3B). The stability of the PPy/GCE and Co/PPy/GCE was examined and compared over a large number of charge–discharge cycles at the current density of 1 A·g^{-1}. According to $C_a = 2(t_2\text{-}t_1)\ I/(u\ s)$, the specific capacitance of nanomaterials have been calculated (see the supporting material for the notes of each physical quantity in the formula). Figure S3B shows that the specific capacitance of the PPy/GCE floats in the range of 71.32 ~ 78.12 F g^{-1}, and the specific capacitance of the Co/PPy/GCE fluctuates in the range of 101.77 ~ 110.08 F g^{-1}. PPy nanocones maintained 91.29% of the original capacitance value after charging and discharging for 100 times, while Co/PPy/GCE maintained 92.45% of the original capacitance value. These results demonstrated that Co/PPy/GCE had a large specific capacitance and excellent cycle stability. This excellent electrochemical property was attributed to the following reasons: (i) PPy nanocone arrays can effectively assist the electron exchange and improve the efficiency of electrolyte ion diffusion; (ii) Hierarchical Co/PPy hybrids with 3D nanostructure provided the large electroactive surface area.

Electrochemical catalysis of nitrite oxidation

The electrocatalytic oxidation of nitrite by Co/PPy/GCE was investigated by CV. As shown in Fig. 4, in 0.2 M PBS (pH 8.0), the PPy/GCE exhibited no obvious electrochemical peak in the absence of nitrite. A typical oxidation peak was observed for Co/GCE and Co/PPy/GCE in the potential range from 0.4 to 1.0 V. Among the three modified electrodes (PPy/GCE, Co/GCE, and Co/PPy/GCE), the catalytic current of Co/PPy/GCE to nitrite increased the most (curve b, Fig. 4). Notably, the 3D nanostructure arrays of Co/PPy can enhance the diffusion of nitrite to the electroactive sites to participate in electrochemical determination [41]. To investigate the transport characteristics of Co/PPy/GCE, CVs were performed at different scan rate in in PBS (pH 8.0) containing 0.01 mM sodium nitrite (Figure S4). A linear equation $y = 328.8\ x$—60.74 ($R^2 = 0.996$) was obtained, where y is the anodic current (Ip), and x is the square root of scan rate ($v^{1/2}$). The result suggested that the oxidation of nitrite on the modified electrode was controlled by diffusion process [42].

According to the existing research results, it is inferred that the electrocatalytic oxidation of nitrite on the modified electrode is an electrochemical and chemical catalytic process [43, 44]. According to the electrochemical oxidation mechanism of Co/PPy, the oxidation mechanism of nitrite on its surface was speculated as follows. Equation 1 and 2 reveal the interaction between Co/PPy nanomaterials and

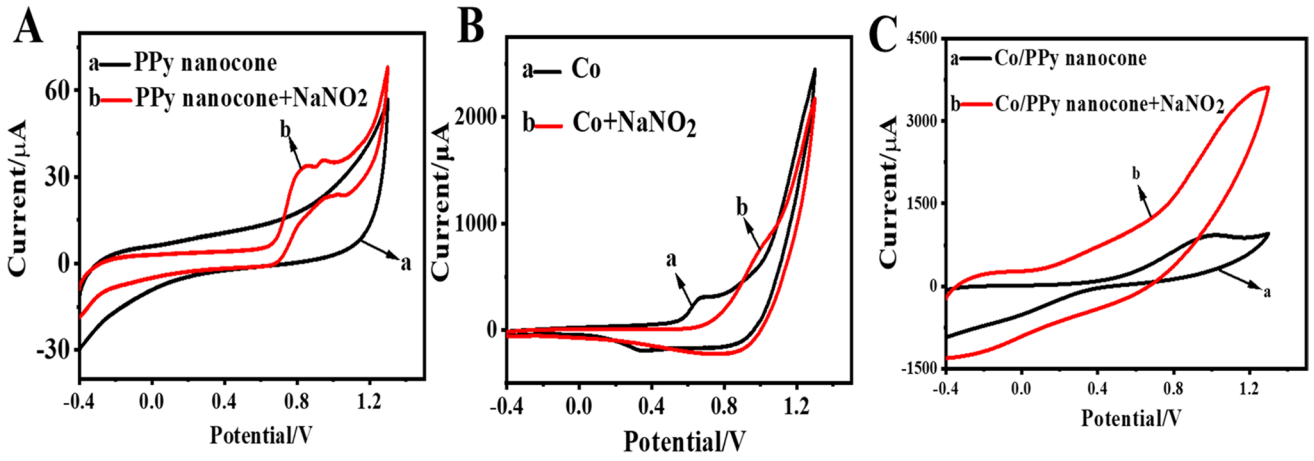

Fig. 4 CVs of PPy/GCE (A), Co/GCE (B), and Co/PPy/GCE(C)in the absence (a) and presence (b) of 0.1 mM sodium nitrite in PBS (pH 8.0) recorded at 0.10 V s^{-1}

nitrite and the production process of nitrogen dioxide (NO_2). Equations 3 and 4 tell why nitrate (NO_3^-) is the only final oxidation product [43–45].

$$\frac{\text{Co}}{\text{PPy}} + NO_{2^-} = [(\text{Co/PPy}) \cdot NO_{2^-}] \quad (1)$$

$$[(\text{Co/PPy}) \cdot NO_{2^-}] = \text{Co/PPy} + NO_2 + e^- \quad (2)$$

$$2NO_2 + H_2O = NO_{3^-} + NO_{2^-} + 2H^+ \quad (3)$$

$$NO_{2^-} + H_2O = NO_{3^-} + 2H^+ + 2e^- \quad (4)$$

Optimization of current response on Co/PPy/GCE

In order to increase the catalytic oxidation properties of Co/PPy/GCE, various factors (the deposition time of Co and voltage, the detection potential, and the pH value of solution) were optimized. Different deposition time of Co nanomaterials can result in various amounts of Co nanomaterials onto PPy nanocones, which can generate different catalytic activities to nitrite. Figure S5 shows the effect of the cobalt deposition time towards the oxidation of nitrite. The amperometric response decreases as the deposition time increases. When the depositing time was 300 s, PPy nanocones had been completely covered with Co nanoparticles. When the deposition time was more than 300 s, the agglomerated Co particles weaken its catalytic ability. Therefore, the best deposition time of Co nanomaterials was 300 s. Figure S5B shows that when the deposition potential of cobalt is − 1.0 V, the current response of sodium nitrite reaches the maximum. As shown in Figure S5C, the oxidation current response of nitrite on the modified electrode increased with the increase of applied potential from 0.45 to 0.65 V, reaching the maximum at 0.55 V. In that way, the optimum potential for the nitrite detection was chosen as 0.55 V. At the same time, the pH value of buffer for the detection of nitrite was optimized, and the current responses were the highest when the pH value was 8.0 (Figure S5D).

Amperometric detection of nitrite

Sodium nitrite was continuously injected into the continuously stirred PBS buffer (pH 8.0) at the same interval, and the amperometric measurement was performed at 0.55 V on Co/PPy/GCE. When sodium nitrite was added to the continuously stirred PBS solution, the current increased sharply until it reached a constant value [46]. And the response time of the modified sensor was within 4 s (reach the 90% steady-state response, left inset of Fig. 5A), which was much quicker than those of previous reports about nitrite sensors [37, 40], showing the fast response. The Co/PPy/GCE exhibited high catalytic activity to the nitrite oxidation. Notably, a linear relationship was observed between the current change (ΔI) and nitrite concentration with the regression equation of $\Delta I/\mu A = 0.1838\ c/\mu M + 8.208$ ($R^2 = 0.993$) (Fig. 5B). The sensor examined a linear range of 2 to 3318 μM nitrite with a sensitivity of 2.60 μA μM^{-1} cm^{-2}, and the detection limit of 0.35 μM (S/N = 3). The excellent performance of Co/PPy/GCE such as low detect limit and fast response time has been compared with the previous sensors, as shown in Table S2. Such excellent sensing performance can be attributed to the following reasons. Firstly, the microstructure of the Co nanoparticles and PPy nanocones ensured that nitrite can diffuse to the electrode interface in a short time. Both PPy nanocones and Co nanoparticles have been proved to be catalytic property towards nitrite oxidation and have synergistic effect. Secondly, through a convenient electrochemical

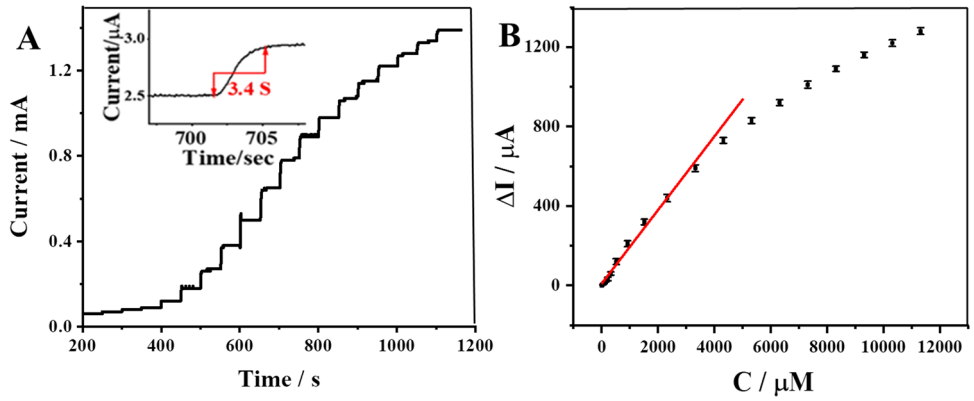

Fig. 5 **A** Amperometric response of Co/PPy/GCE to successive injection of nitrite. The sodium nitrite concentration injected was 2.0, 6.0, 10.0, 20.0, 40.0, 60.0, 80.0, 100.0, 200.0, 300.0, 400.0, 600.0, 800.0, and 1000.0 (repeat nine times) μM in sequence. Inset upper, typical response time; inset lower, enlarged view of i-t curve. **B** Calibration curve of the current response to nitrite concentration at the modified electrode

deposition technique, the surface of the sensor was modified with the Co/PPy nanocone arrays without using any immobilized matrix, so that the Co/PPy was closely connected with the electrode.

The selectivity and stability of the sensor

Possible common coexisting interferences with nitrite at Co/PPy/GCE have been examined by comparing the amperometric response. Figure 6 shows that common potential interferences with nitrite in real samples have also been investigated. Interfering substances included inorganic compounds (KCI, NaCl, $CuSO_4$, $CaCl_2$, sodium citrate) and a wide range of organic compounds (including sucrose, maltose, fructose, glucose, ascorbic acid, lactic acid, acetic acid, and natural phenol rutin). The concentrations of all interferences were 1.0 mM. No significant interference for the detection of 10 μM nitrite was observed. Therefore, the sensor can be selective to common interfering substances.

The long-term stability of the sensor was investigated by recording the current response to nitrite (10.0 μM). The current response of nitrite remained 92.19% after 31 days, indicating that the sensor had good long-term stability (Fig. 6B). The relative standard deviation (RSD) was 3.5%

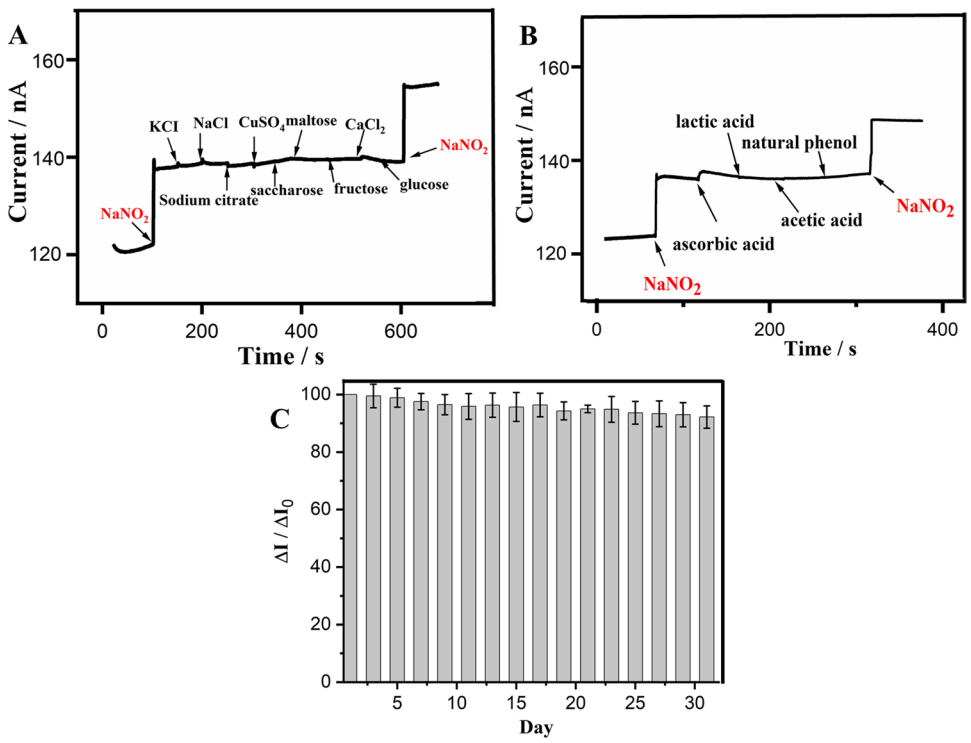

Fig. 6 **A** and **B** The amperometric response of Co/PPy/GCE towards nitrite and interferences. The concentration of nitrite was 10 μM, while the concentrations of all interferences were 1.0 mM. **C** The long-term stability of the sensor towards 5.0 μM nitrite over 31 days

Table 1 Results for determination of nitrite in pickled Chinese cabbage (Wujiang Brand)

Sample	Nitrite measured with this sensor (mg kg^{-1}) [n]	Nitrite measured with a spectrophotometer (UV2501PC) (mg kg^{-1})	RSD (%)
1	0.573	0.555	4.98
2	0.587	0.578	4.78
3	0.629	0.601	5.32

$n = 5$, the detection times of nitrite using this sensor

for 8 consecutive determinations of 10.0 μM nitrite using the same sensor. RSD of 10.0 μM nitrite for six independent sensors was 4.5%. The results showed that the repeatability of inter-electrode and intra-electrode was good.

The real sample assay

Nitrite in pickled Chinese cabbage (Wujiang Brand) was determined by Co/PPy/GCE (produced in Chongqing, China). Under optimal conditions, the sample (pickled juice, 10 μl) was continuously added to the continuously stirred PBS 8.0 solution. The national food hygiene standard set that the content of nitrite in pickles should not exceed 20 mg kg^{-1}, and that in natural vegetables should not exceed 3 ~ 5 mg kg^{-1}. Table 1 shows that the results of the sensor were basically consistent with those of spectrophotometry. At the same time, the sensor has been used for the determination of sodium nitrite in different water samples (Table S3).

Conclusion

PPy nanocone arrays were prepared by template free using an electrochemical polymerization technique, and the formation mechanism and excellent electrochemical properties were highlighted in this work. The obtained PPy nanocones could be wrapped by Co nanoparticles through in situ electrodepositing. A sensitive electrochemical nitrite sensor was developed based on hierarchical Co/PPy nanocone array. Owing to the large electroactive area, the large specific capacitances, and the synergistic effect of the nanocomposite, the Co/PPy-modified sensor showed good electrochemical catalytic property towards nitrite oxidation. These results show that Co/PPy/GCE has a good application prospect for the determination of nitrite in future.

Supplementary Information The online version contains supplementary material available at https://doi.org/10.1007/s00604-021-05131-2.

Funding This work was funded by the National Natural Science Foundation of China (21705088), the National Key Technology R&D Program of China (2017YFD0501500), Shandong Key Laboratory of Biochemical Analysis (SKLBA2008), Shandong Province Agricultural Application Technology Innovation Project (SD2019NJ001-2), and College Students' innovation project (S202010435051).

Declarations

Conflict of interest The authors declare no competing interests.

References

1. Honikel KO (2008) The use and control of nitrate and nitrite for the processing of meat products. Meat Sci 78(1–2):68–76
2. Jonvik KL, Nyakayiru J, Pinckaers PJ, Senden JM, van Loon LJ, Verdijk LB (2016) Nitrate-rich vegetables increase plasma nitrate and nitrite concentrations and lower blood pressure in healthy adults. J Nutr 146(5):986–993
3. Ma L, Hu L, Feng X, Wang S (2018) Nitrate and nitrite in health and disease. Aging Dis 9(5):938–945
4. Parvizishad M, Dalvand A, Mahvi A H, Goodarzi F (2017) A review of adverse effects and benefits of nitrate and nitrite in drinking water and food on human health. Health Scope, In Press
5. Li S, Li J, Zhang B, Li D, Li G, Li Y (2017) Effect of different organic fertilizers application on growth and environmental risk of nitrate under a vegetable field. Sci Rep 7(1):17020
6. Lewis WM, Morris DP (1986) Toxicity of nitrite to fish: a review. Transactions of the American Fish Soc 115(2):183–195
7. Sastry KV, Moudgal RP, Mohan J, Tyagi JS, Rao GS (2002) Spectrophotometric determination of serum nitrite and nitrate by copper-cadmium alloy. Anal Biochem 306(1):79–82
8. Miranda KM, Espey MG, Wink DA (2001) A rapid, simple spectrophotometric method for simultaneous detection of nitrate and nitrite. Nitric Oxide 5(1):62–71
9. Revsbech NP, Nielsen M, Fapyane D (2020) Ion selective amperometric biosensors for environmental analysis of nitrate, nitrite and sulfate. Sensors (Basel) 20(15)
10. Najdenkoska A (2016) Development of HPLC method for analysis of nitrite and nitrate in vegetable. J Agric Food Environ Sci 67:33–39
11. Su Z, Wang X, Luo M, Li L, Tu Y, Yan J (2019) Fluorometric determination of nitrite through its catalytic effect on the oxidation of iodide and subsequent etching of gold nanoclusters by free iodine. Mikrochim Acta 186(9):619
12. Jian J-M, Fu L, Ji J, Lin L, Guo X, Ren T-L (2018) Electrochemically reduced graphene oxide/gold nanoparticles composite modified screen-printed carbon electrode for effective electrocatalytic analysis of nitrite in foods. Sens Actuators, B 262:125–136
13. Zhou Y, Ma M, He H, Cai Z, Gao N, He C, Chang G, Wang X, He Y (2019) Highly sensitive nitrite sensor based on AuNPs/RGO nanocomposites modified graphene electrochemical transistors. Biosens Bioelectron 146:111751
14. Lu L (2019) Highly sensitive detection of nitrite at a novel electrochemical sensor based on mutually stabilized Pt nanoclusters doped CoO nanohybrid. Sens Actuators, B 281:182–190
15. Ye D, Luo L, Ding Y, Chen Q, Liu X (2011) A novel nitrite sensor based on graphene/polypyrrole/chitosan nanocomposite modified glassy carbon electrode. Analyst 136(21):4563–4569
16. Hua Bai GS (2007) Gas sensors based on conducting polymers. Sensors 7:267–307

17. Ibanez JG, Rincon ME, Gutierrez-Granados S, Chahma M, Jaramillo-Quintero OA, Frontana-Uribe BA (2018) Conducting polymers in the fields of energy, environmental remediation, and chemical-chiral sensors. Chem Rev 118(9):4731–4816
18. Zarras P, Anderson N, Webber C, Irvin DJ, Irvin JA, Guenthner A, Stenger-Smith JD (2003) Progress in using conductive polymers as corrosion-inhibiting coatings. Radiat Phys Chem 68(3–4):387–394
19. Umoren SA, Solomon MM (2019) Protective polymeric films for industrial substrates: a critical review on past and recent applications with conducting polymers and polymer composites/nanocomposites. Prog Mater Sci 104:380–450
20. Moon JM, Thapliyal N, Hussain KK, Goyal RN, Shim YB (2018) Conducting polymer-based electrochemical biosensors for neurotransmitters: a review. Biosens Bioelectron 102:540–552
21. Nambiar S, Yeow JT (2011) Conductive polymer-based sensors for biomedical applications. Biosens Bioelectron 26(5):1825–1832
22. Li J, Qiao J, Lian K (2020) Hydroxide ion conducting polymer electrolytes and their applications in solid supercapacitors: a review. Energy Storage Mater 24:6–21
23. Meng Q, Cai K, Chen Y, Chen L (2017) Research progress on conducting polymer based supercapacitor electrode materials. Nano Energy 36:268–285
24. Stejskal J (2019) Interaction of conducting polymers, polyaniline and polypyrrole, with organic dyes: polymer morphology control, dye adsorption and photocatalytic decomposition. Chem Pap 74(1):1–54
25. Kamalabadi M, Mohammadi A, Alizadeh N (2016) Polypyrrole nanowire as an excellent solid phase microextraction fiber for bisphenol A analysis in food samples followed by ion mobility spectrometry. Talanta 156–157:147–153
26. Hui N, Wang J (2017) Electrodeposited honeycomb-like cobalt nanostructures on graphene oxide doped polypyrrole nanocomposite for high performance enzymeless glucose sensing. J Electroanal Chem 798:9–16
27. Yang L, Wang H, Lu H, Hui N (2020) Phytic acid functionalized antifouling conducting polymer hydrogel for electrochemical detection of microRNA. Anal Chim Acta 1124:104–112
28. Wang X, Tan W, Ji H, Liu F, Wu D, Ma J, Kong Y (2018) Facile electrosynthesis of nickel hexacyanoferrate/poly(2,6-diaminopyridine) hybrids as highly sensitive nitrite sensor. Sens Actuators, B 264:240–248
29. Nguyen-Thanh D, Frenkel AI, Wang J, O'Brien S, Akins DL (2011) Cobalt–polypyrrole–carbon black (Co–PPY–CB) electrocatalysts for the oxygen reduction reaction (ORR) in fuel cells: composition and kinetic activity. Appl Catal B 105(1–2):50–60
30. Wang HNM, Yana Z, Denga L, Heb J, Houc Y, Jianga Y, Yu G (2013) Cobalt/polypyrrole nanocomposites with controllable electromagnetic properties. Nanoscale 1:1-7
31. Iqbal J, Numan A, Ansari M O, Jagadish P R, Jafer R, Bashir S, Mohamad S, Ramesh K, Ramesh S (2020) Facile synthesis of ternary nanocomposite of polypyrrole incorporated with cobalt oxide and silver nanoparticles for high performance supercapattery. Electrochim Acta 348
32. Wang H, Lu H, Yang L, Song Z, Hui N (2020) Glycyrrhiza polysaccharide doped the conducting polymer PEDOT hybrid-modified biosensors for the ultrasensitive detection of microRNA. Anal Chim Acta 1139:155–163
33. Meng F, Shi W, Sun Y, Zhu X, Wu G, Ruan C, Liu X, Ge D (2013) Nonenzymatic biosensor based on Cu(x)O nanoparticles deposited on polypyrrole nanowires for improving detection range. Biosens Bioelectron 42:141–147
34. Ozcan L, Sahin Y, Turk H (2008) Non-enzymatic glucose biosensor based on overoxidized polypyrrole nanofiber electrode modified with cobalt(II) phthalocyanine tetrasulfonate. Biosens Bioelectron 24(4):512–517
35. Qu L, Shi G, Yuan J, Han G, Chen F (2004) Preparation of polypyrrole microstructures by direct electrochemical oxidation of pyrrole in an aqueous solution of camphorsulfonic acid. J Electroanal Chem 561(none):149–156
36. Fakhry A, Cachet H, Debiemme-Chouvy C (2015) Mechanism of formation of templateless electrogenerated polypyrrole nanostructures. Electrochim Acta 179:297–303
37. Csisza'r A S c M, To¨ lgyesi M, Mechler A', Nagy JB, Nova'k M (2000) Electrochemical reactions of cytochrome c on electrodes modified by fullerene films. J Electroanal Chem 497:69-74
38. Ren S, Guo Y, Ma S, Mao Q, Wu D, Yang Y, Jing H, Song X, Hao C (2017) Co 3 O 4 nanoparticles assembled on polypyrrole/graphene oxide for electrochemical reduction of oxygen in alkaline media. Chinese J Cata 38(7):1281–1290
39. Khoder R, Korri-Youssoufi H (2020) E-DNA biosensors of M. tuberculosis based on nanostructured polypyrrole. Mater Sci Eng 108:110371
40. Mandler D (2010) Fritz Scholz (Ed.): Electroanalytical methods. Guide to experiments and applications, 2nd ed. Anal Bioanal Chem 398(7–8):2771–2772
41. Yang L, Wang H, Lu H, Hui N (2019) Phytic acid doped poly(3,4-ethylenedioxythiophene) modified with copper nanoparticles for enzymeless amperometric sensing of glucose. Microchim Acta 187(1):49
42. Xia C, Wang N, Lin G (2009) Facile synthesis of novel MnO2 hierarchical nanostructures and their application to nitrite sensing. Sens. Actuators, B 137(2):710–714
43. Madhu R, Veeramani V, Chen SM (2014) Heteroatom-enriched and renewable banana-stem-derived porous carbon for the electrochemical determination of nitrite in various water samples. Sci Rep 4:4679
44. Wang J, Hui N (2017) A nanocomposite consisting of flower-like cobalt nanostructures, graphene oxide and polypyrrole for amperometric sensing of nitrite. Microchim Acta 184(7):1–8
45. Metters J, R. K, C. B, (2012) Electroanalytical properties of screen printed graphite microband electrodes. Sens Actuators B 169:136–143
46. Li J, Yuan R, Chai Y, Zhang T, Che X (2010) Direct electrocatalytic reduction of hydrogen peroxide at a glassy carbon electrode modified with polypyrrole nanowires and platinum hollow nanospheres. Microchim Acta 171(1–2):125–131